



Spectroscopic Investigations of Multi Walled Carbon Nanotubes Functionalized with L-Leucine

Milton Franklin Benial A*, CMS Anandhi

Department of Physics, NMSSVN College, Madurai, Tamilnadu, India

ABSTRACT

In this study, the oxidized Multi Walled Carbon Nanotubes (MWCNTs) were functionalized with the simplest essential amino acid L-Leucine by ultra-sonication process. The structural, optical, morphological and vibrational characterizations of oxidized and L-leucine Functionalized MWCNTs (F-MWCNTs) were carried out by X-Ray Diffraction (XRD), Ultraviolet-Visible Spectroscopy (UV-Vis), Scanning Electron Microscopy (SEM), Energy Dispersive X-Ray analysis (EDX), Fourier Transform Infrared (FTIR) spectroscopy Raman spectroscopy and Electron paramagnetic resonance spectroscopic techniques. The observed spectral features like peak position, intensity, diameter of the nanotubes, crystallinity, were investigated. The various spectral results confirm the successful functionalization of the L-leucine on the outer surface of the MWCNTs. The shift and the broadening of peak in the XRD pattern indicate that the incorporation of L-leucine decreases the crystalline nature. FTIR study confirms the presence of functional groups in oxidized MWCNTs and F-MWCNTs. Raman studies reveals that the functionalization rate is increased due to the higher relative intensity ratio of the F-MWCNTs. EPR study revealed that the EPR absorption data found to be best fit for the Gaussian line shape. The g-value indicates that the system was found to be isotropic in nature. These spectroscopic investigations may lead to the enhancement of the biocompatibility of the f-MWCNTs, which may be useful for further chemistry with various biomolecules in the field of biomedicine and targeted drug delivery.

Keywords: Functionalization; MWCNTs; Leucine; EPR; XRD; Isotropic

INTRODUCTION

Carbon Nanotubes (CNTs), one of the interesting and versatile research material since its discovery by Iijima in 1991 [1]. The intensive experimental and theoretical research of CNTs opens up many new applications in chemistry, electronics, material science and biomedicine. CNTs exist in two forms depending upon their wall structure (i) Single Walled Carbon Nanotubes (SWCNTs), a graphene sheet rolled up into a

cylinder with a diameter of few nanometers and (ii) Multi Walled Carbon Nanotubes (MWCNTs), an arrangement of coaxial graphene sheets from two to fifty numbers [2]. The CNTs possess unique mechanical, electronic, optical, geometric and biological properties [3]. Due to these extraordinary properties and their ability to obtain desired functional groups on their outer surfaces, CNTs have potential applications in various fields like biosensors, nano electronics, molecular transporters, cancer therapy, diagnostics and

Received:	02-October-2021	Manuscript No:	IPNNR-21-10884
Editor assigned:	05-October-2021	PreQC No:	IPNNR-21-10884 (PQ)
Reviewed:	19-October-2021	QC No:	IPNNR-21-10884
Revised:	20-September-2023	Manuscript No:	IPNNR-21-10884 (R)
Published:	27-September-2023	DOI:	10.0.12769/IPNNR.23.7.23

Corresponding author Milton Franklin Benial A, Department of Physics, NMSSVN College, Madurai, Tamilnadu, India; E-mail: miltonfranklin@yahoo.com

Citation Benial MFA, Anandhi CMS (2022) Spectroscopic Investigations of Multi Walled Carbon Nanotubes Functionalized with L-Leucine. J Nanosci Nanotechnol Res. 7:23.

Copyright © 2023 Benial MFA, et al. This is an open-access article distributed under the terms of the Creative Commons Attribution License, which permits unrestricted use, distribution, and reproduction in any medium, provided the original author and source are credited.

targeted drug delivery. In recent years, CNTs have attracted much attention in pharmacological and toxicological aspects. The CNTs are more dynamic in their biological application when compared to other nanomaterials. CNTs can be used not only in imaging but also in drug delivery and thermal ablation while Nanomaterials like quantum dots can be used only in cancer cell imaging [4]. The high aspect ratio and the needle like tube structure of the CNTs makes it a potential carrier of large loads of multifunctional therapeutics, including drugs, genes and targeting molecules along the longitude of the tubes without affecting their cell penetrating capability. The high surface area along with strong mechanical properties and electrical conductivity, CNTs serve as outstanding material for nano scaffolds and three dimensional nano-composites [5]. Moreover, it was found that the purified MWCNTs act as most efficient scavengers of radical oxygenated species [6]. Purification of CNTs eliminates the metal impurities, which are inherent in the pristine CNTs. The oxidation process of the CNTs involve the addition of oxygen containing groups like the carboxyl and hydroxyl functional groups promotes the exfoliation of the CNT bundles and their dispersibility in polar media. Oxidation process converts the hydrophobic property of the CNTs to hydrophilic nature [7]. Functionalization of CNTs enhances the biocompatibility. Functionalization is generally done in two ways (i) Covalent functionalization (ii) Non-covalent functionalization [8]. Covalent functionalization is carried out by the covalent attachment of the chemical groups on the surface of the MWCNTs which is tightly glued to the skeleton of MWCNTs and well matched in a wet environment. Whereas the non-covalent type deals with the wrapping of functional molecules in which the attachment of function groups is mainly due to the thermal conductivity of MWCNTs. The covalent functionalization has the advantage that the attachment of organic moieties occurs either at the tips or the sidewalls of the tubes which can be further utilized for post derivatization furnishing advanced CNT based hybrid materials [9]. Amino acids provide hydrogen bonds and electrostatic interactions for effective lyophilisation [10]. L-Leu is used in the biosynthesis of proteins. It is a ketogenic amino acid that can be degraded directly into Acetyl-CoA which is the precursor of ketone bodies. Acetyl-CoA participates in many biochemical reactions in protein, lipid and carbohydrate metabolism. Its main function is to deliver acetyl group to the Krebs cycle for energy production. This current work focuses on the functionalization of MWCNTs with an essential aliphatic amino acid L-Leucine (Leu).

MATERIALS AND METHODS

Chemicals

The analytical grade chemicals like Sulphuric acid and nitric acid, MWCNTs with 99% purity and L-Leu with 99% purity were purchased and used as received from Sigma Aldrich chemical Co, St. Louis, MO, USA.

Experimental Methods

Oxidation of MWCNTs: The oxidation of MWCNTs was performed by the previously reported procedure [11]. Pristine MWCNTs were mixed in the ratio of 3:1 concentrated sulphuric and nitric acid and sonicated for 3 hours at 40°C in an ultrasonic bath to introduce carboxylic acid groups on the surface of MWCNTs [12]. After sonication, the mixture was added drop wise to cold distilled water and the resulting samples, oxidized MWCNTs, were filtered and dried in vacuum at 80°C for 4 hours.

Functionalization of MWCNTs with L-Leucine: Schematic representation of functionalization process is given in [Figure 1](#). Oxidized MWCNTs were functionalized with 0.1 M, 0.3 M and 0.5 M L-Leucine as given below. Oxidized MWCNTs powder (25 mg) was dispersed in 250 mL of double distilled water and solicated at room temperature for one hour to obtain homogenous solution. The L-Leucine solution was added and sonicated for 30 min followed by 2 hrs of stirring for MWCNTs. The MWCNTs so obtained were thoroughly washed with double distilled water under centrifugation at 10,000 x g for 10 min and the solution phase was discarded. This washing was repeated 5 times in order to remove unbound L-Leucine. The obtained functionalized MWCNTs dried in ambient atmosphere and stored in the refrigerator. The resulting L-Leucine functionalized MWCNTs is denoted as f-MWCNTs respectively in this manuscript [13].

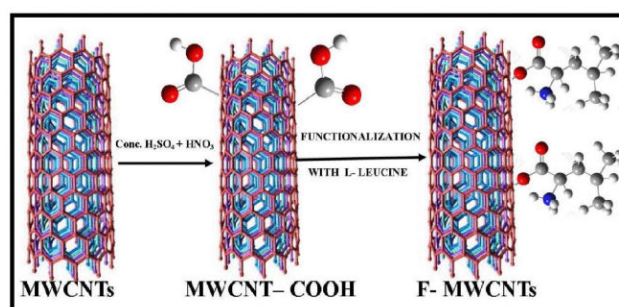


Figure 1: Schematic representation of functionalization process.

Characterization Techniques

XRD experimental analysis was carried out using analytical (Eindhoven, the Netherlands) diffract mowrtdyt,ter under ambient conditions. The tube voltage was maintained as 40 KV and the tube current as 30 mA. A copper target at a wavelength of $k\text{ Cu } K\alpha = 1.54$ and tube voltage of 40 KV and tube current of 30 mA was maintained. The average scanning range and time for the sample was between 10° and 90° of 2 hrs. The rectangular pellets were prepared using the compression mounding. The UV-spectra of the f-MWCNTs were obtained using Shimadzu UV-3600 UV-Vis-NIR spectrophotometer with a wavelength range of 200-400 nm with ethanol as a solvent. The morphology of oxidized and f-MWCNTs were investigated using the SEM-VEGA3 TESCAN, USA. The chemical composition of oxidized MWCNTs and f-MWCNTs were characterized by an energy dispersive spectrometer (Bruker, Nano, Germany). A computerized

Bruker FT-IR spectrometer (Model: Vertex 70) with wavelength range of 400 to 4000 cm^{-1} with the resolution of 4 cm^{-1} was used to obtain FT-IR transmittance spectra. The Raman spectra were recorded from Jobin Yvon Horibra LABRAM-HR visible (400 nm-1100 nm) micro Raman spectrometer with the spectral resolution is of the order 1 cm^{-1} with the range of 50 cm^{-1} to 4000 cm^{-1} . Bruker EMX plus spectrometer with 100 kHz field modulation frequency and phase sensitive detection is used to record. The EPR spectra was recorded by varying the magnetic field in the range of 337 mT-362 mT with the field modulation amplitude 0.6 mT; conversion time, 30 ms; radio frequency power, 5.0 mW; receiver gain, 2000; sweep width, 25 mT; sweep time, 30 s; number of scans, 16; 1024 k resolution; and radiofrequency, 9.86 GHz. The temperature was controlled using a controller with water as a coolant.

RESULTS AND DISCUSSION

Functionalization of MWCNTs with L-Leu an essential amino acid leads to the condensation reaction between the carboxyl acid group in the oxidized MWCNTs and the amino group present in the L-Leu which converts the carboxylic acid into amide resulting the attachment of L-Leu on the MWCNTs. The amino acid functionalized MWCNTs are extensively used in the attachment of various biomolecules like DNA and proteins.

XRD studies

Figure 2 illustrates the XRD patterns of oxidized MWCNTs and 0.1 M, 0.3 M and 0.5 M concentrations of f-MWCNTs. The characteristic peak for oxidized MWCNTs appears at the position $2\theta=25.92^\circ$ and that of 0.1 M, 0.3 M and 0.5 M concentrations of f-MWCNTs appear at $2\theta=26.22^\circ$, $2\theta=26.37^\circ$ and $2\theta=26.54^\circ$ respectively. The characteristic peak value attributes to the (002) diffraction plane of the graphite relating to the interlayer spacing of carbon atoms [14]. The Full Wave Half Maximum (FWHM) of complete XRD spectra is listed in **Table 1**. The FWHM and the crystallinity of CNTs are always inversely proportional to each other. In this paper, the

FWHM increases as the concentration of the L-Leu is increased. This result suggests that the crystallinity decreases due to the attachment of L-Leu on the surface of MWCNTs [15]. The XRD analysis of the f-MWCNTs shows very little changes when compared with the oxidized MWCNTs. Hence, the structure of MWCNTs is not destroyed completely by the acid treatment of the oxidation process and also by the functionalization process [16]. The intensity of the characteristic peak of the f-MWCNTs slightly decreases with the increase of the L-Leu concentration. Hence, the XRD experimental studies validate the successful attachment of the L-Leu to the oxidized MWCNTs by functionalization.

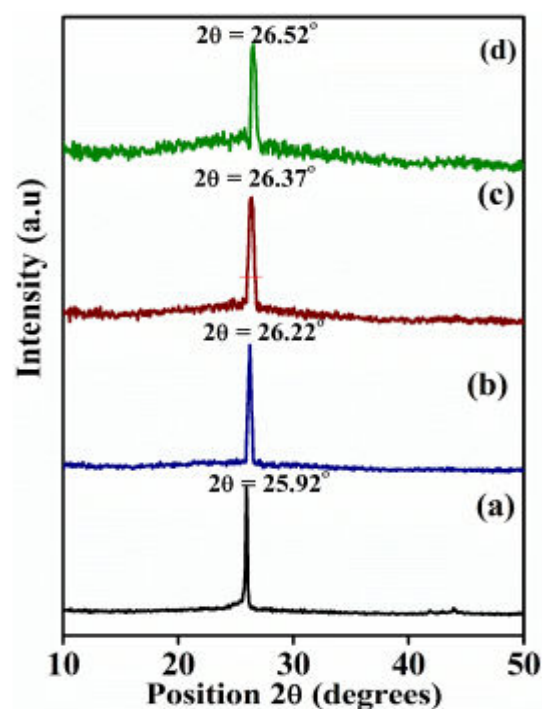


Figure 2: XRD Pattern of (a) oxidized MWCNTs, (b) 0.1 M; (c) 0.3 M; (d) of 0.5 M concentration of f- MWCNTs.

Table 1: XRD assignments of oxidized MWCNTs and 0.1, 0.3 and 0.5 M concentrations of f-MWCNTs.

S.N	MWCNTs	$2\theta^\circ$	FWHM (degree)
1	Oxidized MWCNTs	25.92	0.166
2	f- MWCNTs	0.1 M	26.22
		0.3 M	26.37
		0.5 M	26.54

Optical Properties by UV-Vis Spectral Analysis

UV-Vis analysis is widely used to find the sample purity. The absorption intensity is proportional to the amount of sample dissolved in the solution. UV-Vis spectra of oxidized and f-MWCNTs are shown in Figure 3. The characteristic peak of oxidized MWCNTs and f-MWCNTs peaks are observed at 272 nm, 253 nm, 254 nm and 255 nm respectively. These peaks are due to the π plasmons of free electron cloud in the nanotube. When the nanotubes are formed by rolling the graphene sheet, the π and σ orbitals are not be orthogonal to each other since they tend to hybridize and modify their structure. These facts are predicted by π band model. Thus, it is evident that diameter is inversely proportional to the curvature of the nanotube. The smaller the diameter, the curvature is larger and larger hybridization. The energy of the optical transition is found to be 4.56 eV, 4.87 eV, 4.88 eV and 4.90 eV respectively. From the UV-Vis spectral data, the optical transitions of oxidized and f-MWCNTs are mainly due to the π plasmons caused by π - π^* transition since the energy region is low (0-8 eV). The shift obtained in the absorption peak of f-MWCNTs with respect to oxidized MWCNTs clearly confirms the efficient functionalization of L-Leu on the MWCNTs surface.

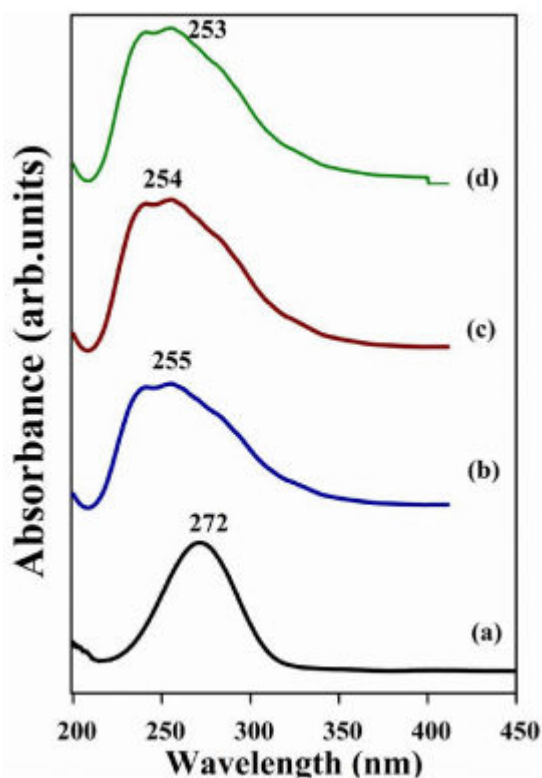


Figure 3: UV Spectra of (a) oxidized MWCNTs; (b) 0.1 M; (c) 0.3 M; (d) of 0.5 M concentration off-MWCNTs.

SEM Imaging and EDX Analysis

Figure 4 shows the SEM images of the oxidized MWCNTs and f-MWCNTs and their corresponding histograms. SEM analysis

is mainly used to characterize the surface morphology of the MWCNTs. The SEM micrographs indicate uniform dispersion of the f-MWCNTs. The SEM images show isolated straight nanotube bundles of oxidized and f-MWCNTs with an average diameter 47±1 nm for oxidized MWCNTs and 65±4 nm for f-MWCNTs given by the corresponding histograms. The diameters of the f-MWCNTs are increased when compared with the oxidized MWCNTs, which represents the successful functionalization of the L-Leucine on the MWCNTs surface. The EDX spectra give the elemental composition of the functional groups present in the sample. The EDX spectra of the f-MWCNTs show the presence of nitrogen whereas the oxidized MWCNTs do not possess the elemental nitrogen. The presence of nitrogen atoms paves the way for the formation of pentagons and hexagons which naturally increases the reactivity of the neighboring carbon atoms. This confirms the attachment of the L-Leu on the MWCNTs surface.

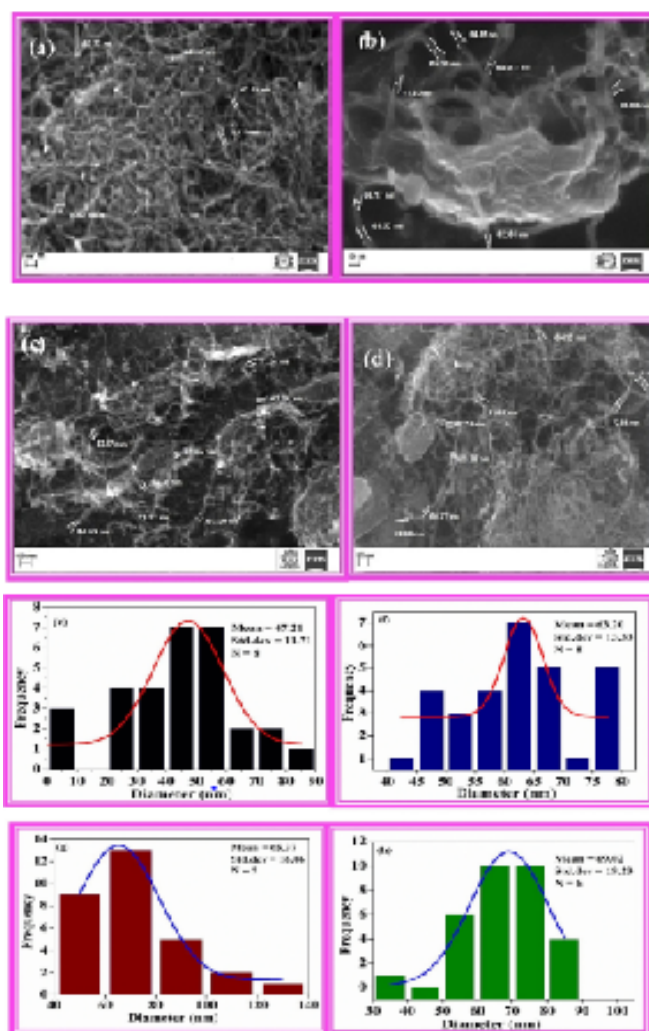


Figure 4: SEM images of (a) oxidized MWCNTs; (b) 0.1 M; (c) 0.3 M; (d) of 0.5 M concentrations of f-MWCNTs and corresponding histograms of SEM images of; (e) oxidized MWCNTs; (f) 0.1 M; (g) 0.3 M; (h) 0.5 M concentration of f-MWCNTs; (h) EDX spectra off-MWCNTs.

FT-TR Spectroscopy

FT-IR spectroscopy is widely used spectroscopic technique for the evaluation the functional groups present in the sample. **Figure 5** presents the FT-IR spectra of oxidized MWCNTs and f-MWCNTs respectively. The characteristic peak was observed at 1582, 1584 and 1587 cm^{-1} , which corresponds to the asymmetric vibration of COO^- . The dipolar nature of the L-Leu is justified by the weak absorption band at 2130, 2132 and 2136 cm^{-1} which attributes to the NH frequencies of 3 ions. The peaks at 2846, 2854, 2858 cm^{-1} are attributed to the aliphatic C-H stretch superimposed on N-H stretch.

The complete assignments of the oxidized MWCNTs and f-MWCNTs are tabulated in **Table 2** respectively. Thus, the FT-IR spectra reveal that the L-Leu is successfully attached to the surface of the MWCNTs.

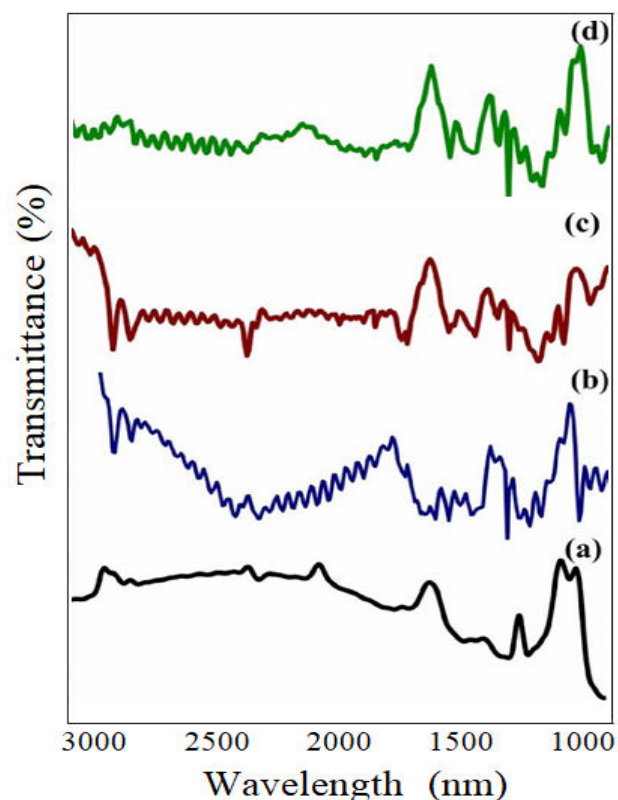


Figure 5: FTIR spectra of (a) oxidized MWCNTs; (b) 0.1 M; (c) 0.3 M; (d) of 0.5 M concentration of f-MWCNTs.

Table 2: Infrared spectral assignments of oxidized MWCNTs and 0.1, 0.3 and 0.5 concentrations of f-MWCNTs.

Assignment	Oxidized MWCNTs wavenumber (cm^{-1})	Assignment	f-MWCNTs with Leucine concentration wavenumber (cm^{-1})		
			0.1 M	0.3 M	0.5 M
C=O stretching	1747	Symmetric bending of CH_3	1310	1311	1319
C=OH Stretching	1630	CH_2 wagging motion	1361	1363	1365
C-H stretching	2927	CH_2 deformation motion	1386	1389	1390
O-H stretching	3437	COO^- stretching	1408	1410	1412
C-O Stretching	1056	Symmetric deformation of NH_3^+	1514	1516	1518
C-OH Stretching	686	Asymmetric stretching of COO^-	1582	1584	1587
		Asymmetric bending of NH_3^+	1607	1609	1611

Combination band of NH_3^+	2132	2134	2136
	2621	2632	2641
	2738	2742	2746
Symmetric stretching of CH_2	2846	2854	2858
Asymmetric stretching of CH_2	2916	2924	2946
Asymmetric stretching of NH_3^+	3062	3064	3066

Raman Spectroscopic Analysis

Raman spectroscopic analysis is a typical non-destructive tool to analyse the crystalline and amorphous carbon atoms in the MWCNTs. It provides a quantitative assessment structural disorder and the amorphous carbon present in the MWCNTs. Raman spectra of the oxidized MWCNTs and the f-MWCNTs with 0.1 M, 0.3 M and 0.5 M concentrations were shown in Figure 6 and their related Raman assignments are presented in Table 3. The MWCNTs has a disorder or defect D band between the region 1320 cm^{-1} -1370 cm^{-1} which is related to the amount of disorder in the MWCNTs and tangential stretching G band around the region 1530 cm^{-1} -1610 cm^{-1} , which corresponds to the tangential in plane vibrations of C-C bonds of the grapheme structure.

The second order weaker band may also occur in the range of 2662-2692 cm^{-1} the amount of disorder is quantitatively analyzed by using the ratio of relative intensities (I_{Dc}). The level of functionalization was estimated by the relative intensity ratio. The higher the relative intensity signifies the good extent of functionalization. In the present studies, the relative intensity ratio increases as the concentration of the L-Leu increases which implies that the functionalization rate is increased by increasing the concentration.

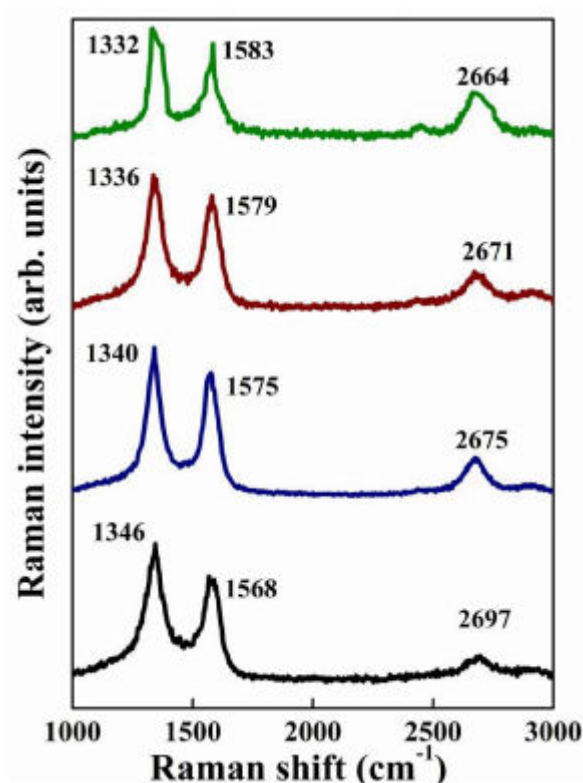


Figure 6: Raman spectra of (a) oxidized MWCNTs; (b) 0.1 M; (c) 0.3 M; (d) of 0.5 M concentration of f MWCNTs.

Table 3: Raman spectral assignments of oxidized MWCNTs and 0.1, 0.3 and 0.5 M concentrations of f-MWCNTs.

MWCNTs	Concentration	D band (cm^{-1})	G band (cm^{-1})	2D band (cm^{-1})	I_{Dc} ratio
Oxidized MWCNTs		1346.55	1568.05	2697.96	1.291
L-Leu Functionalized MWCNTs	0.1 M	1340.56	1575.83	2675.09	1.307
	0.3 M	1336.58	1579.69	2671.71	1.315
	0.5 M	1332.61	1583.56	2664.94	1.325

EPR Spectroscopy

Electron paramagnetic spectroscopy is commonly employed to study the presence of unpaired electrons in the sample. The resonance spectra of carbon based materials such as graphite, amorphous carbon films, fullerenes, carbon nanoparticles and carbon nanotubes are located very close to the free electron g factor value (g factor=2.0023). The EPR spectra of oxidized MWCNTs and 0.1 M, 0.3 M and 0.5 M concentration of f-MWCNTs with their corresponding absorption spectra and Gaussian fit are given **Figure 7**. The g -factor value was calculated using the magnetic field B_0 obtained from the central position of EPR spectral line. The observed EPR parameters like R^2 from Gaussian fit; spin concentration, FWHM and g -factor are tabulated in **Table 4** respectively. The g -factor shows strong shift from the oxidized MWCNTs indicates the presence of unpaired electrons, which strongly suggests the covalent attachment of the L-Leu on the surface of the MWCNTs. The g -factor of oxidized MWCNTs and f-MWCNTs are 2.0115, 2.183, 2.185 and 2.186 respectively. These g -factor values are closer to the free electron g -factor values, which show that the system remains isotropic. The entire system is independent of magnetic field due to the isotropic nature. The larger shift in the g -factor is due to the interaction of L-Leu molecules with the defect sites on the

surface of the MWCNTs. The line shape of the oxidized MWCNTs and f-MWCNTs shows Gaussian line shape, which can be explained in terms of the FWHM the increase in the FWHM values illustrates the line width broadening due to the dipolar interaction.

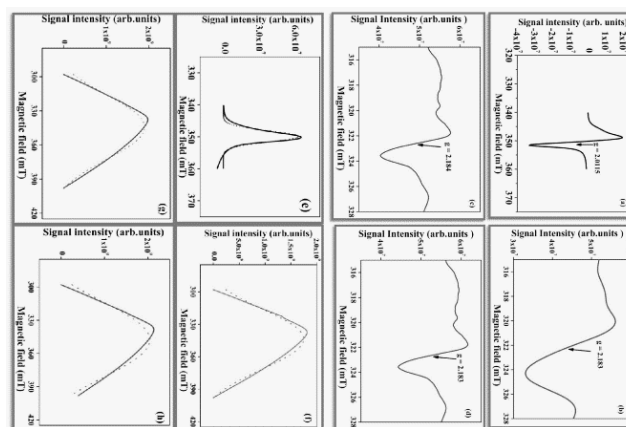


Figure 7: EPR Spectra of (a) oxidized MWCNTs; (b) 0.1 M; (c) 0.3 M; (d) of 0.5 M concentration of f-MWCNTs and corresponding absorption spectra of (e) oxidized MWCNTs; (f) 0.1 M; (g) 0.3 M; (h) 0.5 M concentration of F-MWCNTs and their Gaussian fit.

Table 4: EPR parameters of oxidized MWCNTs and 0.1, 0.3 and 0.5 M concentrations of f- MWCNTs.

MWCNTs	Concentration	R^2 from Gaussian fit	Spin concentration A from Gaussian fit (au)	FWHM (mT)	g -factor
Oxidized MWCNTs		0.97034	2.759×10^8	3.92	2.0115
f-MWCNTs	0.1 M	0.97481	1.427×10^{11}	34.71	2.183
	0.3 M	0.97595	1.610×10^{11}	65.77	2.185
	0.5 M	0.97751	2.439×10^{11}	66.78	2.186

CONCLUSION

The structural, optical, vibrational, morphological and magnetic investigations of oxidized and f-MWCNTs were carried out. The UV-Vis spectral data shows the optical transitions of oxidized and f-MWCNTs are mainly due to the π plasmons caused by π - π^* transition. The surface morphology was analyzed by the SEM micrographs which indicate the uniform dispersion of the f-MWCNTs. The EDX of the f-MWCNTs shows the presence of nitrogen whereas the oxidized MWCNTs do not possess the elemental nitrogen in the EDX analysis. FTIR study confirms the presence of functional groups in oxidized MWCNTs and f-MWCNTs. Raman studies reveals that the functionalization rate is increased due to the higher relative intensity ratio of the f-MWCNTs. EPR study revealed that the EPR absorption data found to be best fit for the Gaussian line shape. The g -value indicates that the system was found to be isotropic in nature. These spectroscopic investigations may lead to the enhancement of the biocompatibility of the f-MWCNTs, which may be useful

for further chemistry with various biomolecules in the field of biomedicine and targeted drug delivery.

ACKNOWLEDGEMENT

The authors thank the management for their encouragement to carry out this work. Financial support from UGC (University Grants Commission) under the scheme of Rajiv Gandhi national fellowship 2016-2017 (Award letter no. F117.1/2016-17/RGNF-2015-17-SC-TAM-27556/(SA-III/Website), Dated 08-January-2016) is highly acknowledged.

REFERENCES

1. Iijima S (1991) Helical microtubules of graphitic carbon. *Nature*. 31:354-356.
2. Iijima S, Ichihashi T (1993) Single shell carbon nanotubes of 1 nm diameter. *Nature*. 363:603.

3. Branch C, Frusteri F, Magazu V, Mangione V (2004) Characterization of carbon nanotubes by TEM and infrared spectroscopy. *J Phys Chem B*. 108:3469-3473.
4. Madani SY, Naderi N, Aaron Tan OD, Seifalian AM (2011) A new era of cancer treatment: carbon nanotubes as drug delivery tools. *Int J Nanomed*. 6:2963-2979.
5. Sadeh H, Shahryari-ghoshekandi R. Functionalization of carbon nanotubes and its application in nanomedicine: A review. *Nanomed J*. 2:231-248.
6. Fenoglio I, Tomatis M, Lison DJ, Muller A (2006) Reactivity of carbon nanotubes: Free radical generation or scavenging activity? *Biol Med*. 40:1227.
7. Fayazfar H, Afshar A, Dolati A, Dolati M (2013) DNA impedance biosensor for detection of cancer, TP53 gene mutation, based on gold nanoparticles/aligned carbon nanotubes modified electrode. *Sci Appl*. 4:667-678.
8. Singh P, Campidelli S, Giordani S, Bonifazi D, Bianco A, et al. (2009) Organic functionalisation and characterization of single walled carbon nanotubes. *Chem Soc Rev*. 38: 2214-2230.
9. Chronopoulos DD, Kokotos CG, Karousis N, Kokotos G, Tagmatarchis N, et al. (2015) Functionalized multi walled carbon nanotubes in an aldol reaction. *Nanoscale*. 7:2750-2757.
10. Mohammed AR, Coombes AGA, Perrie Y (2007) Amino acids as cryoprotectants for liposomal delivery systems. *Eur J Pharm Sci*. 30: 406-413.
11. Anandhi CMS, Benial AMF (2019) Bio functionalization of multi-walled carbon nanotubes with L-Alanine. *Mater Res Express*. 6: 115625.
12. Ramanathan T, Fisher FT, Ruoff RS, Brinson LC (2005) Amino functionalized carbon nanotubes for binding to polymers and biological systems. *Chem Mater*. 17: 1290-1295.
13. Rance GA, Marsh DH, Nicholas RJ, Khlobystov AN (2010) UV-vis absorption spectroscopy of carbon nanotubes: Relationship between the π -electron plasmon and nanotube diameter. *Chem Phys Lett*. 493:19-23.
14. Guo GY, Chu KC, Ding-sheng W, Chun-gang D (2004) Linear and nonlinear optical properties of carbon nanotubes from first principles calculations. *Phys Rev*. 69:205416.
15. He RR, Jin HZ, Zhu J, Yan YJ, Chen XH (1998) Physical and electronic structure in carbon nanotubes. *Che Phys Lett*. 298:170-176.
16. Wang CH, Dub HY, Sai YTT, Chenc CP, Huang CJ, et al. (2007) High performance of low electro catalysts loading on CNT directly grown on carbon cloth for DMFC. *J Power Sources*. 171:55-62.